TOPOLOGY OPTIMIZATION OF 2D TRUSSED STRUCTURES

F. A. C. Martins

M. A. Silva

flavio.martins@aluno.ufabc.edu.br

marcelo.araujo@ufabc.edu.br

Centro de Engenharia, Modelagem e Ciências Sociais Aplicadas – CECS, Universidade Federal do ABC – UFABC.

Alameda da Universidade, 09606-045, São Paulo, São Bernardo do Campo, Brasil.

Abstract. *In this work an optimization process is applied on a 2D truss subjected to static forces and self-weight load. The goal of the optimization is to minimize the structure's weight using two separated methodologies. The first one consists on finding the minimum cross-section area for each bar element that is able to resist the loads. Constraints are considered to be the maximum normal stress. In this first part it is used the Simplex method. For the second part, the methodology developed minimizes the structure's mass by shifting its nodes in order to shorten the bar elements. The sequence of nodes that are shifted in the process is made manually, while the algorithm determines when to stop shifting, based on the gradient vector of the constraints' curves. For the optimization of the cross-section area, a new methodology for writing and defining the objective function based on the linearity of the system's equations is proposed.*

Keywords: *Topology optimization; buckling; trussed structures; discrete optimization; aerospace structures.*

INTRODUCTION

Many authors have been working on methods and solutions for minimizing structures' mass. From simple solutions, based on material selection, to sophisticated genetic algorithm, e.g., (RAJAN, 1995), (LINGYUN, 2005) and (STOLPE, 2016), the main goal of the process of optimization is – generally – to find a structure that saves as much material as possible, while preserving its reliability. In this work, particularly, the problem of optimizing a truss will be separated in two well-defined steps: (I) the first one, in which minimal cross-section areas are obtained for the bar elements using a (developed) linear function within a Simplex algorithm; (II) and the second one, that follows from the point that the first one has lead, by shifting the structure's nodes in order to find a geometry that is able to make elements shorter or even eliminate them, creating an optimum topology for the 2D structure.

Although some researches have been done in the same sense, like Wang (2002), that explores the same kind of idea by optimizing the structure's topology, or Croce (2003), that applies genetic algorithm to optimize the structure's volume, there are fewer works nowadays that tries to use original procedures with non-commercial software when dealing with the "minimization of cross section areas", i.e., developing new approaches. Besides that, there are considerable advances in this field for two approaches: (I) by removing or allocating bar elements on the structure, known as "discontinuity layout optimization" (SMITH, 2007), generally applied with finite element analysis (FE) and linear programming; (II) or by removing nodes from a surface that have minor contribution to the stiffness (WALKER, 2016) until a trussed look-a-like shape is obtained.

In this work, particularly, the algorithm it-self takes great attention, since it is not directly based on other codes written before. Therefore, some discussion about the programming process will be made when it becomes necessary. Above all, a new methodology used on the optimization process was developed in order to optimize the cross-section area which avoids the necessity of determining directly the normal forces applied in each normal direction or solving the FE model for each loop.

The contributions of this research are, for the optimization of cross section areas, the development of a linear methodology that eliminates the necessity of recalculating the displacements, deformations and reactions on each iteration. Also, it avoids the obligation of determining algebraically linear equations for the normal tensions for each bar-element; and for the optimization of topology: the development of an algorithm for shifting the free-nodes based on commands given by the user.

1 BACKGROUND

The structure analyzed in this work is the one shown by Fig. 1, with each element and node identification represented.

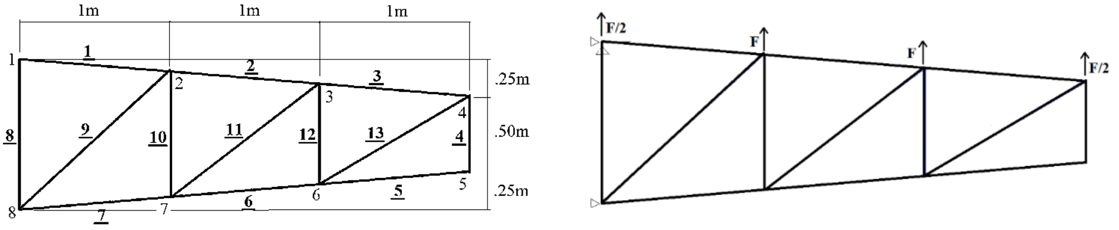

(a) (b)

Figure 1: (a) the original truss model used in this work. (b) external loads and restrictions for the truss tested. The weight of the bars elements are also considered in the model.

The proposed external load is shown by Fig. 1(b). The truss is fixed by node 8, in the vertical and horizontal direction, and it is fixed in the horizontal direction at node 1. For the first optimization procedure, the weight of the structure, W, and an external generic load, F, are considered in the model. In this case, the free variables of the system are the cross-sections areas of the bar element, represented by:

$$\boldsymbol{X}^T = [A_1\ A_2 \ldots A_{13}]^T = [X_1\ X_2 \ldots X_{13}]^T \tag{1.}$$

The objective function is giving by (Farshin, 2010):

$$f(\boldsymbol{X}) = \rho[L_1 A_1 + \cdots + L_{13} A_{13}] = \rho[L_1 X_1 + \cdots + L_{13} X_{13}] \tag{2.}$$

In equation (2), ρ represents the specific mass of the structure, considered to be homogeneous. It is clear from (2) that the objective function represents the total mass of the truss. The restrictions are giving by:

$$\sigma_i \leq \sigma_{adm} \ \rightarrow \ \frac{N_i}{A_i} - \sigma_{adm} \leq 0, \ \ | \ i \in [1, 2, \ldots, 13] \tag{3.}$$

The minimization problem defined by (1), (2) and (3), until this points, express the formulation used by most authors, e.g., (KRIPKA, 2004). For numerically modelling the behavior of the structure the finite element methodology (FEM) was applied. For correctly operating the displacements and forces associated to each bar in global system coordinates, the element' stiffness matrices were computed using:

$$K_i = \frac{E_i A_i}{L_i} \begin{bmatrix} \cos^2(\theta) & \cos(\theta) sen(\theta) & -\cos^2(\theta) & -\cos(\theta)\, sen(\theta) \\ \cos(\theta) sen(\theta) & sen^2(\theta) & -\cos(\theta)\, sen(\theta) & -sen^2(\theta) \\ -\cos^2(\theta) & -\cos(\theta)\, sen(\theta) & \cos^2(\theta) & \cos(\theta)\, sen(\theta) \\ -\cos^2(\theta) sen(\theta) & -sen^2(\theta) & \cos(\theta)\, sen(\theta) & sen^2(\theta) \end{bmatrix} \tag{4.}$$

With the variables shown by Fig. 2.

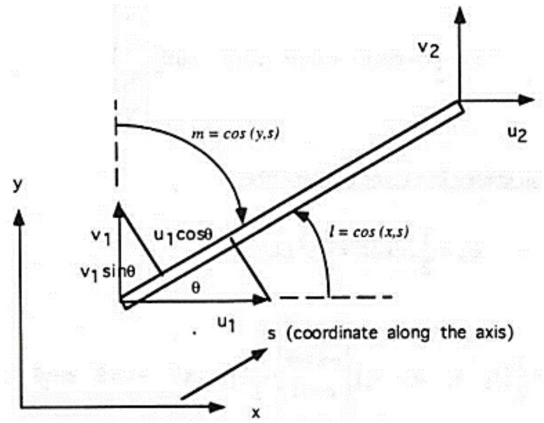

Figure 2: components of the local coordinate system converted to the global one (Logan, 2011).

Giving the components of displacements by the vector $\boldsymbol{u}$, the normal tension applied is calculated by the expression giving by (5). The displacements are obtained from the constitutive equation $\{F_{ext}\} = [K]\{u\}$, for the global stiffness matrix obtained from the superposition of each local stiffness matrix.

$$T_i = \frac{E_i}{L_i}[-\cos(\theta) \quad -\mathrm{sen}(\theta) \quad \cos(\theta) \quad sen(\theta)]\begin{Bmatrix} u_{1x} \\ u_{1y} \\ u_{2x} \\ u_{2y} \end{Bmatrix} \tag{5.}$$

For the first part of the optimization process, the model and constraints described by (1) to (5) are sufficient to determine the problem. For the second optimization part, which involves shifting the nodes of the structure, the bucking effect must be considered. Bucking is going to be caused by a compression load, making it a new restriction for the optimization algorithm:

$$\sigma_{cr} = \frac{P_{cr}}{A} = \left(\frac{1}{A}\right)\frac{\pi^2 EI}{l^2} \tag{6.}$$

From the equation (6) it becomes clear that there are just two ways of dealing with bucking (making the critical load higher): by decreasing the bar's length or by increasing its inertia. As a matter of fact, the first option is the free-variable of system, while the second one will be fixed by considering that the truss is made of circular shapes with different radius – this shape makes the inertia of the area equal in all directions. One other important aspect to notice relies on the inertia associated to the circular shape, given by 7(a) and the area itself, by 7(b), where R represents the external radius and r, the internal, of a bar with tube shape:

$$\begin{aligned} I_c &= \frac{\pi}{4}(R^4 - r^4) \quad (a) \\ A_c &= \pi(R^2 - r^2) \quad (b) \\ A_t &= \pi R^2 \quad (c) \end{aligned} \tag{7.}$$

Noticing that the critical tension will be higher for more eccentric shapes, but at the same time it decreases with area, and that the mass will increase with larger cross-section areas, the obvious solutions becomes: for elements subjected to compression forces, a tube-like cross-section area, A_c, will be used, as seen in 7(b), while for elements subjected to traction, a simple – full – circular area, A_t, is more appropriated, as shown by equation 7(c). In other words, the shapes of the bars will be circular, but for those subjected to compression forces, a tube shape increases the ratio I/A, denoting a more cleaver choice. For the second optimization part – working on the structure's topology – the free variables are described by:

$$\boldsymbol{X}^T = [x_1\ x_2 \ldots x_{13}]^T = [L_1\ L_2 \ldots L_{13}]^T \tag{8.}$$

While the objective function remains the same given by (2), but fixing the areas and making the lengths, L, the free-variables. New restrictions are added to the formulation used in (3), given by:

$$\sigma_i - \frac{\pi^2 E\left[\frac{1}{\pi}(r_2^4 - r_1^4)\right]}{l_i^2 \pi (r_2^2 - r_1^2)} \leq 0 \tag{9.}$$

The restriction in (9) shall only be applied for those elements subjected to compression forces, which the algorithm may be able to identify automatically. By applying this, obtaining too long and thin bar-elements during the evolution of the system is avoided, since the bucking restriction would be reached.

2 METHODOLOGY

2.1 Cross-section areas optimization

For the first part – optimization of the cross section areas – a new methodology was explored: starting from Fig. 3, where the global stiffness matrix is represented, a linear problem is defined by the creation of coefficients that relates the i-th load to the reaction P_{ij} over the j-th bar element using the constitutive equation and the load vector:

$$\begin{aligned} P &= \left[q_{1,x};\ q_{1y};\ q_{2,x};\ q_{2,y}; \ldots; q_{8,x}; q_{8,y}\right] \\ &= \Big[0;\ -\frac{P_1+P_8}{2}+\frac{F}{2};0;\ -\frac{P_1+P_2+P_9+P_{10}}{2} \\ &\quad + F; 0; -\frac{P_2+P_{11}+P_{12}+P_3}{2}; 0;\ -\frac{P_3+P_{13}+P_4}{2} \\ &\quad + \frac{F}{2};\ -\frac{P_5+P_4}{2}; 0; -\frac{P_{12}+P_{13}+P_6+P_5}{2}; 0; -\frac{P_7+P_{10}+P_{11}+P_6}{2}; 0; -\frac{P_8+P_9+P_7}{2}\Big]^T \end{aligned} \tag{10.}$$

K =

1.3268e+07	-1.1057e+06	-1.3268e+07	1.1057e+06	0	0	0	0
-1.1057e+06	6.4236e+06	1.1057e+06	-9.2141e+04	0	0	0	0
-1.3268e+07	1.1057e+06	2.3689e+07	1.3817e+06	-7.0659e+06	5.8882e+05	0	0
1.1057e+06	-9.2141e+04	1.3817e+06	6.8877e+06	5.8882e+05	-4.9069e+04	0	0
0	0	-7.0659e+06	5.8882e+05	1.2462e+07	1.5581e+06	-2.2800e+06	1.9000e+05
0	0	5.8882e+05	-4.9069e+04	1.5581e+06	3.4897e+06	1.9000e+05	-1.5833e+04
0	0	0	0	-2.2800e+06	1.9000e+05	3.9346e+06	7.7462e+05
0	0	0	0	1.9000e+05	-1.5833e+04	7.7462e+05	6.2021e+05
0	0	0	0	0	0	-1.5747e-28	-2.5718e-12
0	0	0	0	0	0	-2.5718e-12	-4.2000e+04
0	0	0	0	-6.2694e-27	-1.0239e-10	-1.6546e+06	-9.6462e+05
0	0	0	0	-1.0239e-10	-1.6721e+06	-9.6462e+05	-5.6237e+05
0	0	-1.4718e-26	-2.4037e-10	-3.1159e+06	-2.3369e+06	0	0
0	0	-2.4037e-10	-3.9255e+06	-2.3369e+06	-1.7527e+06	0	0
-2.3739e-26	-3.8769e-10	-3.3547e+06	-3.0762e+06	0	0	0	0
-3.8769e-10	-6.3315e+06	-3.0762e+06	-2.8209e+06	0	0	0	0

...

...

0	0	0	0	0	0	-2.3739e-26	-3.8769e-10
0	0	0	0	0	0	-3.8769e-10	-6.3315e+06
0	0	0	0	-1.4718e-26	-2.4037e-10	-3.3547e+06	-3.0762e+06
0	0	0	0	-2.4037e-10	-3.9255e+06	-3.0762e+06	-2.8209e+06
0	0	-6.2694e-27	-1.0239e-10	-3.1159e+06	-2.3369e+06	0	0
0	0	-1.0239e-10	-1.6721e+06	-2.3369e+06	-1.7527e+06	0	0
-1.5747e-28	-2.5718e-12	-1.6546e+06	-9.6462e+05	0	0	0	0
-2.5718e-12	-4.2000e+04	-9.6462e+05	-5.6237e+05	0	0	0	0
2.0784e+04	1.7320e+03	-2.0784e+04	-1.7320e+03	0	0	0	0
1.7320e+03	4.2144e+04	-1.7320e+03	-1.4433e+02	0	0	0	0
-2.0784e+04	-1.7320e+03	3.8762e+06	1.1498e+06	-2.2008e+06	-1.8340e+05	0	0
-1.7320e+03	-1.4433e+02	1.1498e+06	2.2499e+06	-1.8340e+05	-1.5283e+04	0	0
0	0	-2.2008e+06	-1.8340e+05	1.2348e+07	3.1063e+06	-7.0311e+06	-5.8593e+05
0	0	-1.8340e+05	-1.5283e+04	3.1063e+06	5.7424e+06	-5.8593e+05	-4.8827e+04
0	0	0	0	-7.0311e+06	-5.8593e+05	1.0386e+07	3.6622e+06
0	0	0	0	-5.8593e+05	-4.8827e+04	3.6622e+06	9.2012e+06

Figure 3: global stiffness matrix for a structure with $E = 210GPa$ and circular cross-section areas with $R_{ext} = 1m^2$.

For the stiffness matrix in Fig. 3, with unitary areas, and the load vector given by equation (10), the influence of each source of load in a specific element of the structure can be computed using:

$$\begin{aligned} &\sigma_1 = c_{10}F + c_{11}W_1 + c_{12}W_2 + \cdots + c_{1n}W_n \\ &\dots \\ &\sigma_i = c_{i0}F + c_{i1}W_1 + c_{i2}W_2 + \cdots + c_{in}W_n \end{aligned} \tag{11.}$$

With this formulation, n vectors filled with coefficients of the influence of each load to the normal tension in a specific element can be directed registered, e.g., applying an external load of $F = 1N$, as represented by Fig. 1(b), will create a coefficient $c_{11} = -4{,}516 \left(\frac{\mathrm{Pa}}{\mathrm{Pa}}\right)$ for the normal tension felt by the element 1, in this case a tension of $-4{,}516Pa$ for each $1N$ applied. Considering only the influence of the 4th bar's weight, $W_4 = 1N$, over the load created on the 1st bar, a tension of $5{,}891\text{x}10^{-16}Pa$ is generated over the element, thus: $\sigma_{14} = \frac{c_{14}W_4}{W_4|_{W_4=1N}} = \left(\frac{c_{14}}{1}\right)W_4 = 5{,}891\text{x}10^{-16}W_4$.

The value of total tension will then be obtained by the sum of all loads contributions, using equation (11). In this case, we define the tension created in each element as a linear addition of every existing source of load on the system, including the structure's weight. Thus, there is no need to compute the forces and reactions multiple times directly from the FE model along the algorithm's loops, being necessary to do so only "n=number of bar" times. The procedure for assembling equation (11) consists on making every other source of load null, while making the i-th equal to one.

The truss used for this work has 13 vectors of loads calculated using equation (11). They are all shown by Table 1, in which is also explicit the source which has originated each vector. Two examples related to the data are shown by Fig. 4 and 5.

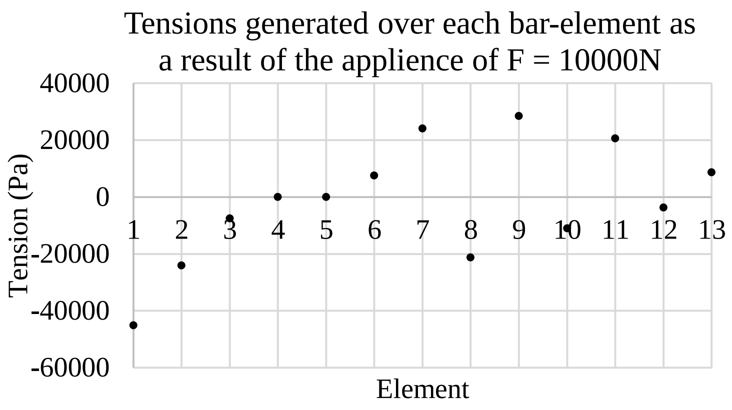

Figure 4: normal tension values generated on each bar element from the appliance of $F = 10000N$

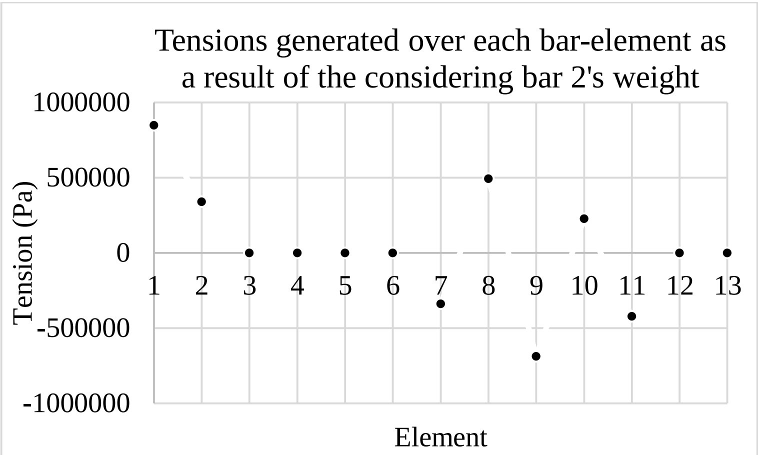

Figure 5: normal tension values generated on each bar element when considering a unitary weight for the bar number 2.

The constraints for the optimization problem are now given by:

$$x_i \geq \sum_{j=0}^{13} \frac{c_{j,i}}{\sigma_{adm}} \left(\frac{\rho L_j x_j}{P_{0,j}} \right) \rightarrow \quad x_i + \sum_{j=1}^{13} \frac{c_j}{\sigma_{adm}} \left(\frac{\rho L_j x_j}{P_{0,j}} \right) \geq \frac{c_0}{\sigma_{adm}} \tag{12.}$$

Table 1: Coefficients of tension associated to each source of force over the i-th element. Each component x_{ij} represents the influence that 1N force related to the j-th source makes over the i-th bar'1s normal tension.

Load:	Vector of coefficients
F = 1N	[-4.515E+00; -2.409E+00; -7.530E-01; 5.891E-16; 2.220E-16; 7.530E-01; 2.409E+00; -2.125E+00; 2.848E+00; -1.100E+00; 2.062E+00; -3.749E-01; 8.686E-01]
Weight of element 1	[4.087E+05; 1.804E-09; 1.077E-09; -1.084E-11; -5.821E-11; -9.459E-10; -1.470E-09; 3.735E+05; -5.526E+05; 4.765E-10; -8.149E-10; 1.085E-11; -1.310E-09]
Weight of element 2	[1.226E+06; 4.906E+05; 4.657E-09; -1.013E-10; 2.910E-11; -4.162E-09; -4.906E+05; 7.130E+05; -9.947E+05; 3.259E+05; -6.111E+05; 3.827E-09; -5.472E-09]
Weight of element 3	[2.044E+06; 1.472E+06; 6.135E+05; -3.679E-10; -1.164E-10; -6.135E+05; -1.472E+06; 6.450E+05; -7.735E+05; 5.703E+05; -1.069E+06; 3.055E+05; -7.077E+05]
Weight of element 4	[1.222E+06; 9.780E+05; 6.114E+05; -2.030E+05; 1.164E-10; -6.114E+05; -9.780E+05; 3.045E+05; -3.303E+05; 2.436E+05; -4.567E+05; 3.044E+05; -7.053E+05]
Weight of element 5	[1.222E+06; 9.780E+05; 6.114E+05; -2.030E+05; 1.164E-10; -6.114E+05; -9.780E+05; 3.045E+05; -3.303E+05; 2.436E+05; -4.567E+05; 3.044E+05; -7.053E+05]
Weight of element 6	[2.044E+06; 1.472E+06; 6.135E+05; -4.074E+05; -2.328E-10; -6.135E+05; -1.472E+06; 6.450E+05; -7.735E+05; 5.703E+05; -1.069E+06; 7.129E+05; -7.077E+05]
Weight of element 7	[1.226E+06; 4.906E+05; 4.773E-09; -9.296E-11; -1.310E-10; -4.424E-09; -4.906E+05; 7.130E+05; -9.947E+05; 7.334E+05; -6.111E+05; 4.074E+05; -5.937E-09]
Weight of element 8	[4.087E+05; 2.008E-09; 1.281E-09; -9.359E-10; -5.821E-11; -1.251E-09; -1.863E-09; 7.809E+05; -5.526E+05; 4.074E+05; -9.313E-10; 9.359E-10; -1.441E-09]
Weight of element 9	[3.638E-10; 2.474E-10; 1.637E-10; 2.071E-12; -1.819E-12; -1.455E-10; -2.351E-10; 4.060E+05; -2.001E-10; 1.143E-10; -8.004E-11; 1.143E-10; -2.183E-10]
Weight of element 10	[3.638E-10; 2.474E-10; 1.637E-10; 2.071E-12; -1.819E-12; -1.455E-10; -2.351E-10; 4.060E+05; -2.001E-10; 1.143E-10; -8.004E-11; 1.143E-10; -2.183E-10]
Weight of element 11	[1.527E+06; 6.111E+05; 5.937E-09; -1.210E-10; -1.455E-10; -5.297E-09; -6.111E+05; 8.882E+05; -1.239E+06; 9.135E+05; -7.613E+05; 1.984E-09; -7.334E-09]
Weight of element 12	[1.085E+06; 6.512E+05; 4.773E-09; -1.173E-10; -8.731E-11; -4.307E-09; -6.512E+05; 4.507E+05; -5.868E+05; 4.326E+05; -8.112E+05; 2.704E+05; -5.588E-09]
Weight of element 13	[2.358E+06; 1.698E+06; 7.077E+05; -4.196E-10; 0.000E+00; -7.077E+05; -1.698E+06; 7.441E+05; -8.923E+05; 6.579E+05; -1.234E+06; 8.224E+05; -8.164E+05]

In (12), $x_i = A_i$ are the free variables of the optimization problem, where, $c_{j,i}$ is the j-th coefficient of influence over i-th element, given by Table 1. $P_{0,j}$, the weight of the j-th element before the optimization process and $(\rho L_j x_j)$, the weight of the same element after the one optimization loop. By using (12), there is no need to directly determine the forces over each element, neither their horizontal or vertical components, making this method more valuable for complex structures or for those that are fulfilled with too many elements, making the task of determining expressions for the normal load exhausting. One numeric example of restriction for the truss shown by Fig. 1 is given by (13), in which the problem becomes that of solving a simple algebraic expression.

$$
\begin{aligned}
x_1 - (-1.514\mathrm{E}-03)x_2 - (-2.524\mathrm{E}-03)\mathrm{x}_3 - (-1.510\mathrm{E}-03)\mathrm{x}_4 \\
- (-2.524\mathrm{E}-03)\mathrm{x}_5 - (-1.514\mathrm{E}-03)\mathrm{x}_6 \\
- (-5.047\mathrm{E}-04)\mathrm{x}_7 - (-4.355\mathrm{E}-19)\mathrm{x}_8 \\
- (-6.824\mathrm{E}-04)\mathrm{x}_9 - (-8.390\mathrm{E}-04)\mathrm{x}_{10} \\
- (-1.886\mathrm{E}-03)\mathrm{x}_{11} - (1.340\mathrm{E}-03)\mathrm{x}_{12} \\
- (-2.912\mathrm{E}-03)\mathrm{x}_{13} \geq 6.359\mathrm{E}-05
\end{aligned}
\tag{13.}
$$

For solving this first part the optimization process it was used the Excel' solver. The algorithm applied to do so was the Simplex, as the problem of minimizing the cross-section areas is linear. To determine the coefficients on Table 1, it was used the Software Matlab with a finite element representation of the given truss. Finally, to prove the results, two simulations of the structure were made using Abaqus: one for the original structure and the other one, after the optimization process.

2.2 Topology optimization

The algorithm developed for this part was created using Matlab, and its diagram is shown by Fig. 6. The main idea is to shift the structures' nodes while minimizing the mass and respecting the constraints given for the problem's formulation. Noticing that, now, one more restriction becomes necessary: the bucking of the elements, as introduced by (6). It must be avoided in order to have feasible results, that is, avoiding creating too long and thin structures that could eventually fit the normal tension criteria. The algorithm created for the procedure works as shown by Fig. 6: the user manually choses a node to be shifted and a direction to do so, then the code will change the topology while the total mass decreases.

The way it notices that the mass is decreasing or increasing is based on the gradient of the mass' curve, that is, the shifting process will continue as long as the mass is decreasing and the restrictions are still being respected; this data will be saved for further analyses. For this part, the optimization process was made by a single algorithm written in Matlab, and the results, proved by simulating and comparing the final and initial structures using Abaqus. The objective function and other mathematic aspects are the ones shown from (1) to (9).

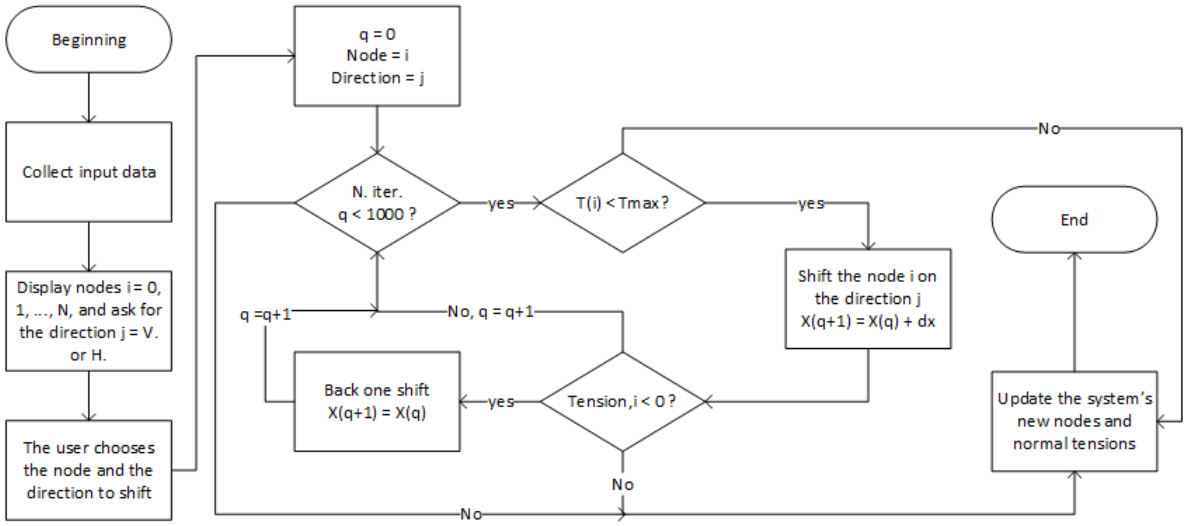

Figure 6: diagram of the topology optimization algorithm.

3 RESULTS

3.1 Results from the cross-section area optimization

For the present analysis, the specific mass and admissible normal tensions are those shown by Table 2. Further, the original areas - used to compute the coefficients c - and optimized ones are also represented.

Table 2: characteristics and results for the optimization of cross section areas.

Characteristics of the optimization problem:
Specific mass: 56200kg/m³; Admissible tension: 562MPa Algorithm: Simplex (Excel' solver)
Areas used for determining the coefficients c:
$A_1 = ... = A_{13} = 1m^2$
Optimized cross-section areas (in order) [m²]:
8.065E-05; 4.296E-05; 1.341E-05; 1.000E-07; 1.000E-07; 1.337E-05; 4.273E-05; 3.809E-05; 5.041E-05; 1.969E-05; 3.661E-05; 6.699E-06; 1.544E-05

The results of mass and tension related to each element are shown by Fig. 7. In Fig. 8, it is shown the original model simulated with Abaqus. The values displayed are in Pa and are related to the appliance of $F = 1N$, with bars of 1m² of cross section areas. The values of tension in such conditions are used to determine the coefficients c_{ij} in (11).

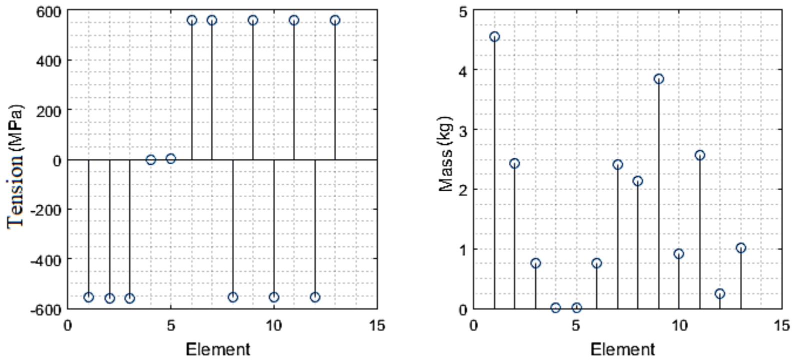

Figure 7: results of the optimization problem: the final mass and normal tension for each element.

After simulating the structure in Abaqus, it becomes clear that the algorithm was able to put the tensions of 11 elements out of 13 as the maximum permitted, while two of them had its components converted to 0, which means that they are not really necessary for the structure. These two elements, at the right end of the truss, are shown in green in Fig. 9. With this results, the first optimization step is finished. Starting from this point, the second optimization part will shift the nodes of the optimized truss in order to improve its topology, further reducing the mass.

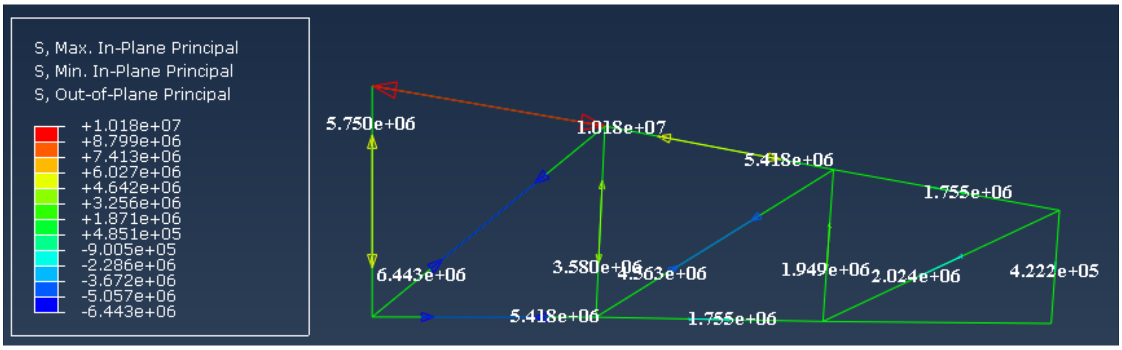

Figure 8: a model of the original structure made with Abaqus for simulating the truss before the optimization process. The values of tension represented in this figure are in Pa. The displacements of nodes are not in scale.

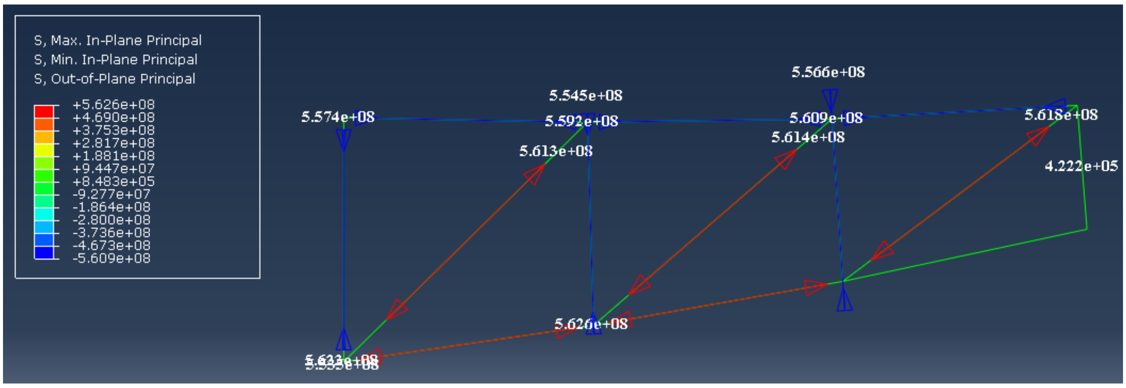

Figure 9: The structure after the optimization process. The tensions represented in the figure are in Pa and the cross section area of each element matches to the ones shown in Table 2. The displacements are in a scale of 1:5,6 to the real values.

3.2 Topology optimization

For this part of the optimization process, the given restrictions, --- characteristics of the bars and the sequence of nodes shifted with the respective directions are shown by Table 3.

Table 3: characteristics of simulation used on the topology optimization process.

Characteristics of the truss and the simulation	$\sigma_{N,max} = 100MPa$ $E = 70GPa$ $\rho = 2700kg$ $F_{ext} = 10000N$
R_2 and R_1 for the tube bars and R for the full-section element.	$r_2 = 0{,}0275m$ $r_1 = 0{,}9r_2$ $r = 0{,}0126m$
Num. max. of loops permitted:	$q = 1000$
Sequence of nodes and directions used:	p_5 *horizontal* p_6 *horizontal* p_6 *vertical* p_5 *horizontal*

From the result shown by Fig. 7 it becomes clear that two bars are not necessary, as they do not contribute to the structure's stiffness. So, before applying the second algorithm, the structure's topology was updated to that represented by Fig. 10. The identification used for the bar-elements, for now on, are the ones shown here. One other important aspect to notice is that only nodes 5 and 6 may be shifted, as 1 and 7 are restricted, and 1, 2, 3, 4 support the external force F.

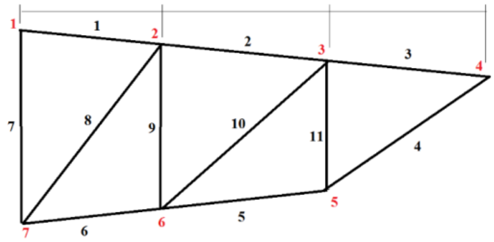

Figure 10: the updated structure used for the second optimization process.

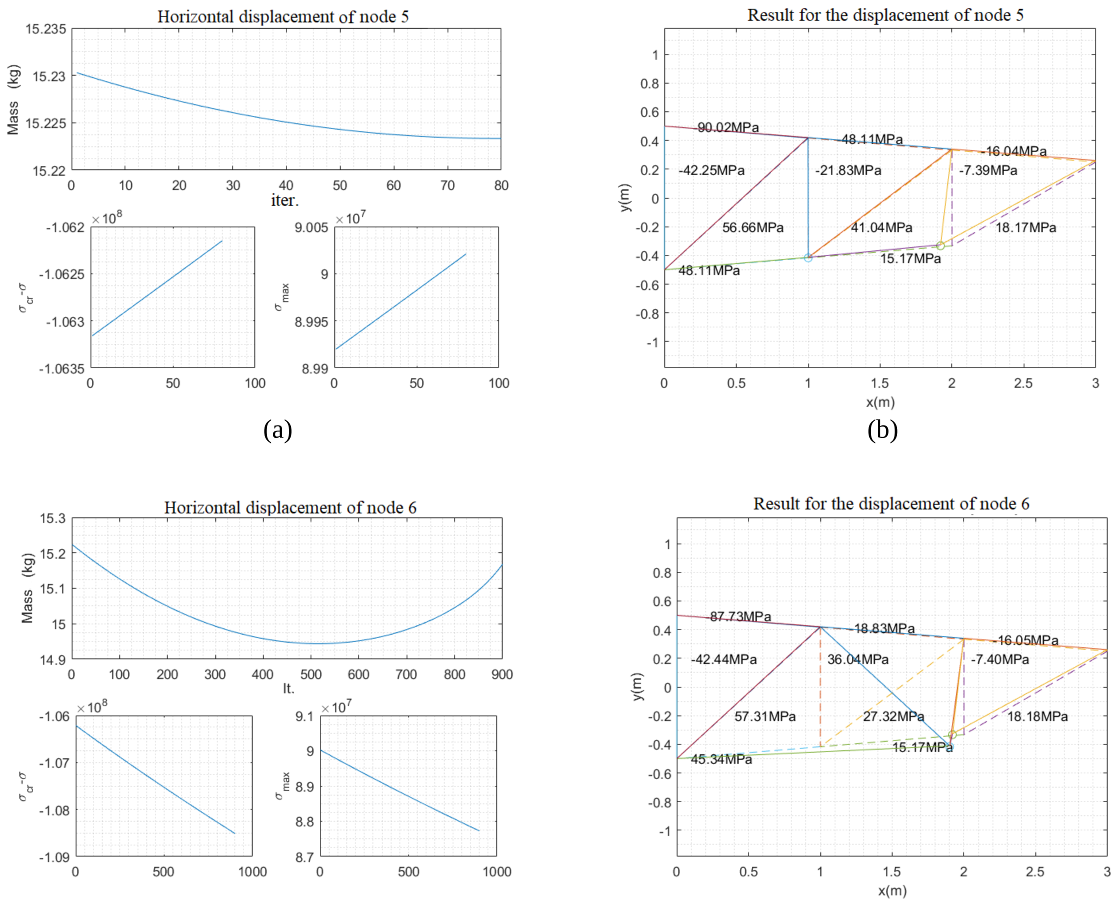

(a) (b)

(c) (d)

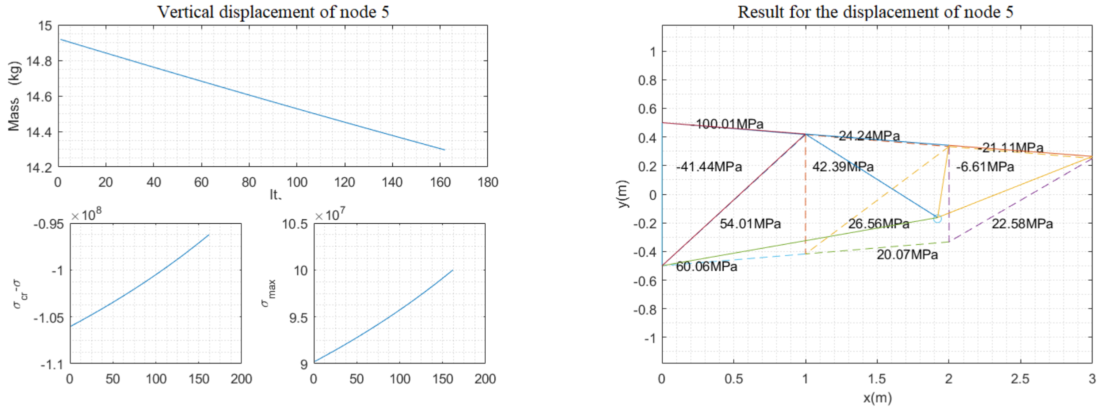

(e) (f)

Figure 11: (left) the changes in mass and margin of normal tensions values. (right) The beam before (dot-line) and after the node shift (continuous-line). Figures (a) and (b) are related to the first procedure, (c) and (d), to the second and (e) and (f), the third, as shown by Table 3.

The new topology is shown by Fig. 11. As it is possible to see, the first bar has the highest compression load, as it was expected, while the bars on the extreme lower part are subjected to tensile. The final tensions values obtained are given by Fig.13. To the left, the values of compression forces, to the right, all tensions values.

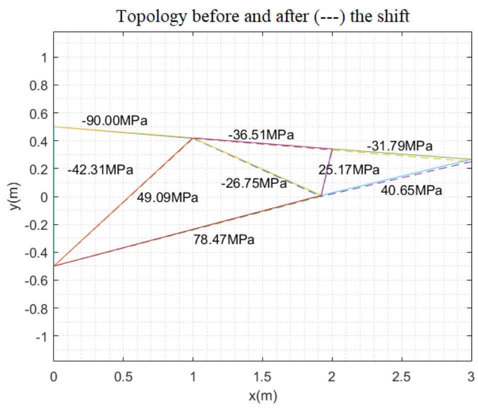

Figure 12: final topology achieved by the structure.

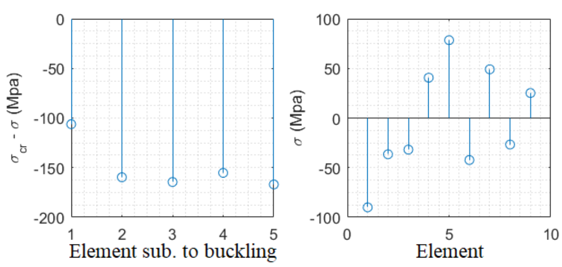

Figure 13: traction and compression tensions' values for each element on the structure.

By comparing the original structure to the last one, represented by Fig. 10 and 12, respectively, the new topology achieved for this systems was able to improve the topology, as the nodes that are not restricted (the ones that support the external forces) got closer to each other, minimizing the cross-area of the structure – its volume – but still being able to support the loads. One other important aspect of this simulation is the fact that the compression forces showed greater influence, as all of the five compressed elements got close to achieve the maximum buckling tension value, while all of them were still far from the yield-tension criteria.

As a matter of fact, the process used until this stage was able to reduce the mass of the optimized structure obtained from the optimization of cross-section areas from 15,26kg to 11,60kg, just by shifting the nodes, reducing it by 23,93%. But, from the results in Fig. 13, there are still room for improvements. The way of doing that is by applying again the algorithm of optimization of cross section areas. By doing that, the mass of the new structure would be improved. Nevertheless, the results obtained from this last process were tested using Abaqus, and the simulation result is shown by Fig. 14.

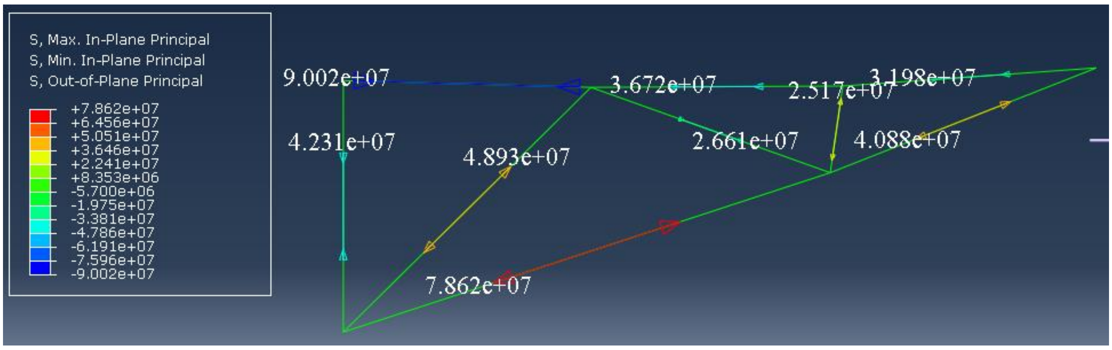

Figure 14: results of the simulation with the final truss' topology simulated with Abaqus.

Although, we have presented a methodology for optimizing the given structure, some other aspects may come in hand for further analysis of viability, e.g., considering dynamic forces and imposing intervals or limits to the frequencies of resonance (GOMES, 2011). One other valuable result would be achieved by applying these techniques over discrete optimization (KOUMOUSIS, 1994).

4 CONCLUSIONS

Starting from a generic truss that was used to resist to external forces and its own weight, we have discussed the optimization of its mass by applying a two-step procedure: first, by minimizing its mass with the reduction of each element's cross-section area and, then, optimizing its topology by shifting its nodes. By doing so, it was achieved a truss with two elements less and a more compact cross area, thus, achieving this work's goal. Furthermore, a new methodology, based on the superposition of effects and the linearity of the load problem was, also, proved to work, which brings within it at least two benefits: removes the necessity of calculating the role structure's response on each loop of the algorithm using FE; and the one of calculating the global and local components of force applied on each element, making the process of simulating complex structure faster. For future works, the possibility of mixing both optimization types used in this work in just one single algorithm would be more appropriated, as the final result would not require the user to try one or another, individually, multiple times in order to further improve the results.

REFERENCES

Behrooz, F & Ali, A., 2010, *Sizing optimization of truss structures by method of centers and force formulation*. *Int. J. Solids. Struct*., vol. 47., n. 18-19, pp 2508-2524

Groce, E., 2003. A Genetic Algorithm for Structural Optimization of Steel.

Kripka, M., 2004, Discrete Optimization of Trusses by Simulated Annealing, *J. Braz. Soc. Mech. Sci & Eng.*, vol. 26, n 2, pp 10-20.

Lingyun, W., Zhao, M., Guangmin, W. and Guang, 2005. M. Truss Optimization on Shape and Sizing with Frequency Constraints Based on Genetic Algorithm. *Comput. Mech.*, vol. 361, n 36, pp 361-368.

Logan, D. L., 2011, A First Couse in the Finite Element Method. *Cengage Learning*.

Rajan , S. D., 1995, Sizing, Shape, and Topology Design Optimization of Trusses Using Genetic Algorithm. *J. Struct. Eng.*, vol. 121, pp 1480-1487.

Smith, C. and Gilbertm M., 2007, Application of Discontinity Layout Optimization of Plane Plasticity Problems. *Proc. R. Soc. A*., vol. 463, pp 2461-2484.

Stolpe, M., 2016, Truss Optimiation with Discrete Design Vareables: a Critical Review. M. *Struct. Multidisc Optim*., vol. 53, n. 2, pp 349-374.

Vlasis, K. and Georgiou, G. P., 1994. Genetic Algorithms in Discrete Optimization of Steel Truss Roofs. *J. Comput. Civil. Eng.*, vol 8, n. 3.

Walker, D. Liu, D. and Jennings, A., 2016, Wing Design Utilizing Topology Optimization and Additive Manufacturing. *Proced. To 57th AIAA Structures, Structural Dynamics, and Materials Conference.*

Wang, D., Zhang, W. H. and Jiang, J. S., 2002. Truss Shape Optimization With Multiple Displacement Constraints. *Comput. Method Appl. M.*, vol. 191, n. 33, pp 3597-3612.